J Appl Electrochem (2009) 39:2521–2528
DOI 10.1007/s10800-009-9946-7

ORIGINAL PAPER

Citrate-based zinc–polyaniline secondary cell: part I: optimization of the citrate/chloride electrolyte

B. Z. Jugović · T. Lj. Trišović · J. S. Stevanović · M. M. Gvozdenović · B. N. Grgur

Received: 12 December 2008 / Accepted: 7 June 2009 / Published online: 19 June 2009

Abstract Electrochemical behavior of zinc and thin polyaniline (PANI) electrodes in citrate/chloride-contained electrolyte has been investigated by the means of electrolyte composition optimization. Electrolyte contained 0.8 M sodium citrate, 0.3 M ammonium chloride, and ~0.3 M zinc chloride has been found to be an optimum electrolyte for the further applications in the real zinc–polyaniline citrate/chloride-based secondary cell.

Keywords Polyaniline · Zinc · Batteries · Citrate · Chloride

1 Introduction

According to the three E′ criteria suggested by Rüetschi and Beck [1, 2], zinc–polyaniline (PANI) secondary cells have some potential advantages, in comparison with classical (protonic and aprotonic) cells, such as ecological acceptability, uses of water-based electrolytes, and relatively low manufacturing costs. The Zn | ammonium chloride, zinc chloride | PANI electrochemical system is one of the most investigated [3], and is based on the following half-cell reactions:

$$[\mathrm{PANI}]_n + ny\mathrm{Cl}^- \underset{\text{Discharge}}{\overset{\text{Charge}}{\rightleftarrows}} \left[\mathrm{PANI}^{y+}(\mathrm{Cl}^-)_y\right]_n + ny\mathrm{e} \quad \text{(Positive electrode)}, \tag{1}$$

where y is the doping degree, and

$$\mathrm{Zn}^{2+-} + 2\mathrm{e} \underset{\text{Discharge}}{\overset{\text{Charge}}{\rightleftarrows}} \mathrm{Zn} \quad \text{(Negative electrode)}. \tag{2}$$

The reaction during charge/discharge of the complete cell can be given as follows:

$$2[\mathrm{PANI}]_n + 2ny\mathrm{Cl}^- + ny\mathrm{Zn}^{2+} \underset{\text{Discharge}}{\overset{\text{Charge}}{\rightleftarrows}} 2\left[\mathrm{PANI}^{y+}(\mathrm{Cl}^-)_y\right]_n + ny\mathrm{Zn}. \tag{3}$$

Such system has been investigated by different authors [3–14]. It was concluded that zinc passivation and dendrite formation, as well as degradation of PANI at higher potentials are the main reasons why this system has not been commercialized till now.

In our previous articles [15, 16], it was shown that citrate/chloride-based electrolyte at pH ~5 has some potential advantages in comparison with pure chloride electrolyte. Due to the complexation of the free zinc ions, citrate anions produce negative shift of the open circuit potentials for more than 100 mV.

On the other hand, decrease of exchange current density and increase of deposition overpotential in chloride/citrate-contained electrolyte lower dendrite formation and probably zinc corrosion rate. In the cycling regime for the anodic potential limit of ~0.35 V (SCE), citrate/chloride electrolytes show better characteristic (higher specific capacity and Columbic efficiency of the PANI electrode) than the

B. Z. Jugović · T. Lj. Trišović
Institute of Technical Science, Serbian Academy of Science and Arts, Knez Mihailova 35, Belgrade, Serbia

J. S. Stevanović
ICTM, Institute of Electrochemistry, Njegoševa 12, Belgrade, Serbia

M. M. Gvozdenović · B. N. Grgur (✉)
Faculty of Technology and Metallurgy, University of Belgrade, Karnegijeva 4, 11020 Belgrade, Serbia
e-mail: BNGrgur@tmf.bg.ac.rs

pure chloride electrolyte. Faster decrease of specific capacity in cycling regime for the anodic potential limits of 0.5 V (SCE) in citrate/chloride than in pure chloride electrolyte has been explained by higher hydrophilic effect of citrate anions. In citrate/chloride electrolyte, it seems that both anions are involved in doping of the PANI film, producing the broad peak. It was suggested that at the less positive potentials, doping proceeds with chloride, and at the more positive potentials with citrate anions, where faster degradation can occur [15].

In this article, we further investigated the behavior of the zinc and PANI electrode in citrate/chloride-contained electrolytes, mainly by the means of the electrolyte composition optimization, with the aim to obtain necessary data for preparation of the real cell, the characteristic of which will be given in the second part of this article.

2 Experimental

The working electrodes, zinc plate ($S = 2$ cm^2), and cylindrically shaped graphite inserted in Teflon holder ($S = 0.64$ cm^2) were mechanically polished with fine emery papers (2/0, 3/0, and 4/0, respectively) and then with polishing alumina (0.05 μm, Banner Scientific Ltd.) on the polishing cloths (Buehler Ltd.). After mechanical polishing, the traces of polishing alumina were removed from the electrode surface in an ultrasonic bath in ethanol during 5 min. For all the experiments, three-compartment electrochemical cells, with platinum foil ($S = 2$ cm^2) as a counter and saturated calomel electrode, $E_r = 0.243$ V (SHE), were used as a reference electrode at room temperature. The electrochemical measurements were carried out using Gammry PC3 and PAR 386 potentiostat/galvanostat controlled by a computer via interface.

Corrosion rate of the zinc electrode was investigated by measuring the mass loss of the polished pure zinc plate ($S = 8$ cm^2) after exposure for over 120 h in 200 ml of the investigated solution.

The zinc deposition efficiency was determined by measuring the mass difference of the polished copper substrate 2 × 2 cm ($S = 8$ cm^2) after zinc deposition, and by applying the Faraday's law. In all the cases, the total deposition charge was the same (50 mA h cm^{-2}). For the current density of 5 mA cm^{-2}, the zinc deposition/dissolution efficiency was determined by measuring the potentials. Micrographs of the zinc deposits at different current densities were obtained with an optical microscope (LEICA-DC 150) connected to the computer.

Polyaniline thin film electrode was obtained from the 1 M hydrochloric acid solution with the addition of 0.25 M aniline monomer (p.a. Merck, previously distilled in the argon atmosphere), at a constant current density of 2 mA cm^{-2} for 1080 s. The total polymerization charge was 0.6 mA h cm^{-2}. After polymerization, the electrode with the current density of 1 mA cm^{-2} was discharged, washed with bidistilled water, and transferred into the second electrochemical cell for further investigations.

All the electrolytes were prepared from p.a. grade chemicals (Merck) and bidistilled water. pH of all the investigated electrolytes was ~5, adjusted by 2 M sodium hydroxide, 1 M hydrochloric, or 1 M citric acid.

3 Results and discussion

3.1 Zinc electrode

3.1.1 Polarization and corrosion measurements

Figure 1 shows the polarization curves for the zinc deposition/dissolution reaction in the electrolytes containing 0.8 M Na-citrate and 0.3 M NH_4Cl with the addition of 0.05, 0.10, 0.30, and 0.50 M $ZnCl_2$ in comparison with the electrolyte containing 0.20 M $ZnCl_2$ + 0.50 M NH_4Cl, at pH ~5.

The zinc deposition/dissolution reaction of the chloride-contained electrolyte was characterized with an open circuit potential of −1 V (SCE) or −0.76 V (SHE), single anodic and cathodic Tafel slopes of ±33 mV dec^{-1}, and exchange current density of ~1.5 mA cm^{-2}. These values provoke the growth of dendrites during deposition reaction, as it is shown in Fig. 2 and explained in more details in Jugović et al. [15].

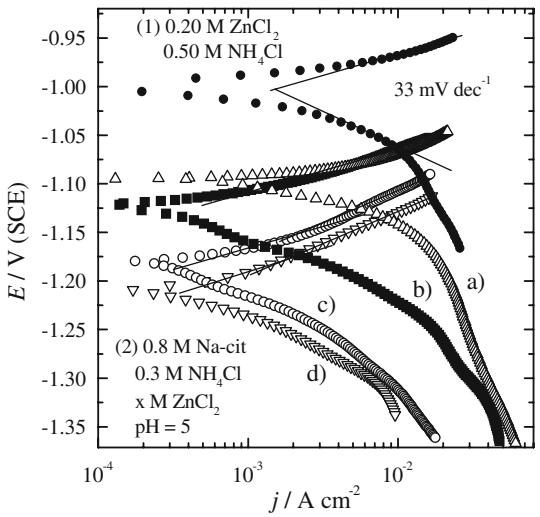

Fig. 1 IR-corrected polarization curve of the zinc electrode in the electrolytes containing (1) 0.5 M NH_4Cl + 0.2 M $ZnCl_2$ and (2) 0.8 M Na-citrate and 0.3 M NH_4Cl with the addition of (a) 0.5, (b) 0.3, (c) 0.1, and (d) 0.05 M $ZnCl_2$

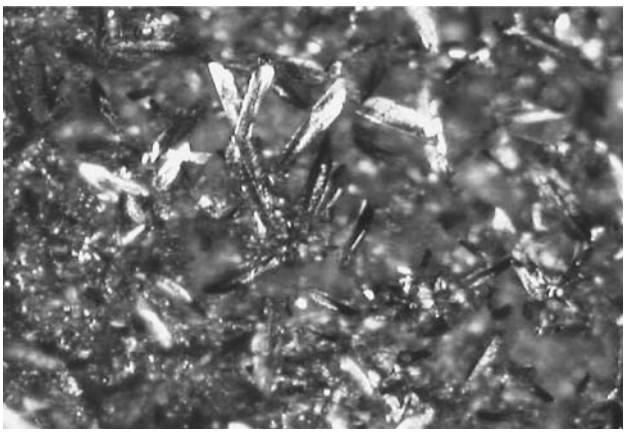

Fig. 2 Micrographs of the zinc deposits from 0.20 M $ZnCl_2$ + 0.50 M NH_4Cl. Deposition current density 3.5 mA cm^{-2}, deposition time 3 h, magnification 100×

Open circuit potential of the zinc electrode in citrate/chloride-contained electrolyte has more negative values in comparison with pure chloride electrolyte, which implies complexation of free zinc ions by citrate anions. For the same current density during polarization, it could be observed that anodic potentials (battery discharge) in citrate/chloride-contained electrolyte were significantly lower than that in the pure chloride electrolyte. This means that discharge voltage in citrate/chloride electrolyte will be higher. On the other hand, due to the more negative cathodic potentials (battery charge) in citrate/chloride electrolyte, charge voltage will be minimum 0.2 V higher than that in the pure chloride electrolyte.

Exchange current density was determined from the intercept of anodic Tafel line with open circuit potentials, since cathodic Tafel line was not well defined. In the separate experiments for all the citrate/chloride-contained electrolytes, the corrosion current density was determined as well. Determined values of equilibrium potentials, and exchange and corrosion current densities were summarized and shown in Table 1.

From the values given in Table 1, it can be observed that open circuit potential, and exchange and corrosion current densities decrease with decreasing zinc chloride concentration. Comparing the values of exchange and corrosion current densities, it can be concluded that the main reactions at the open circuit potential were deposition and dissolution reactions of zinc, while contribution of the corrosion was between 2% and 5%. From these results, it could be suggested that the low concentration of the zinc chloride will be beneficial from the anode point of view. However, on the other hand, under cathodic polarization, low concentration of the zinc chloride provokes relatively low value of the limiting current density. For example, in solution containing 0.05 M $ZnCl_2$, the limiting current density was $\sim$10 mA cm^{-2}, while in the electrolyte containing 0.5 M $ZnCl_2$, the limiting current density was >50 mA cm^{-2}. Hence, based on the values of exchange, and limiting and corrosion current densities, as well as the value of the open circuit potential, the optimum zinc chloride concentration will be $\sim$0.3 M.

Table 1 Determined values of open circuit potentials, and exchange and corrosion current densities of solid zinc electrode for different concentrations of zinc chloride in citrate/chloride-contained electrolytes

$c(ZnCl_2)$/M	E_r/V (SCE)	E_r/V (SHE)	j_0/mA cm^{-2}	j_{corr}/μA cm^{-2}
0.50	−1.094	−0.853	1.0	50
0.30	−1.122	−0.881	0.5	10
0.10	−1.180	−0.939	0.4	9
0.05	−1.209	−0.968	0.3	5

Polarization curve of the solid zinc electrode in the "optimum electrolyte" containing 0.8 M Na-citrate, 0.3 M NH_4Cl, and 0.3 M $ZnCl_2$ is shown in Fig. 3.

Anodic part of the polarization curve was characterized with the single Tafel slope of 60 mV dec^{-1} up to the current densities of 30 mA cm^{-2}. Cathodic part has few not well-defined waves, marked as (a–d), which could be connected with limiting currents. Hence, the value of cathodic Tafel line in this electrolyte cannot be determined. On the other hand, even the overpotential for the hydrogen evolution reaction on zinc is very high; some possibilities that hydrogen evolution could occur exist. At pH $\sim$5, the concentration of the free hydrogen ion corresponds to a negligibly small diffusion limiting current density. However, in the presence of the protonated citrate species (such as $HCit^{2-}$) which could serve as a proton donor, the

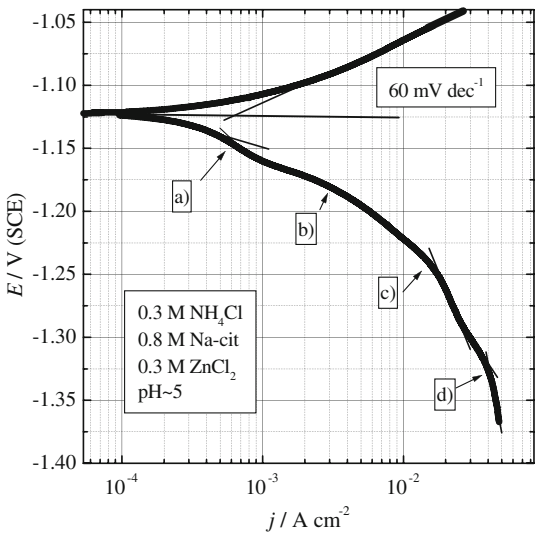

Fig. 3 IR-corrected polarization curve of the zinc electrode in the electrolyte containing 0.8 M Na-citrate, 0.3 M NH_4Cl, and 0.3 M $ZnCl_2$

limiting current density for hydrogen evolution could be significantly higher [17, 18].

For this reason, the influence of deposition current density and morphology on deposition current efficiency was investigated.

3.1.2 Current efficiency and morphology of the zinc deposits

Figure 4 shows determined current efficiency of zinc deposition reaction for the different deposition current densities. Copper substrate was applied to avoid possible oxidation of the zinc substrate which could affect the results, and to determine zinc deposition/dissolution efficiency. In all the cases, the total deposition charge was the same (50 mA h cm^{-2}).

Inset of Fig. 4 shows electrode potentials during zinc deposition. The electrode potentials were similar to the one obtained from polarization curves. For the same current density of 5 mA cm^{-2} dependence of the deposition and dissolution potentials of the zinc on copper over time was measured in order to obtain Columbic efficiency. It was observed that the Columbic efficiency for deposition/dissolution (charge/discharge) reaction was ~100%.

From Fig. 4, one can see that the current efficiency of zinc deposition reaction for low current densities of 2 mA cm^{-2} was relatively small (80%). By increasing the deposition current density to 5 mA cm^{-2}, the current efficiency increases up to 98%. Further increases of the current density provoked a small decrease of the current efficiency, from 97 to 94%.

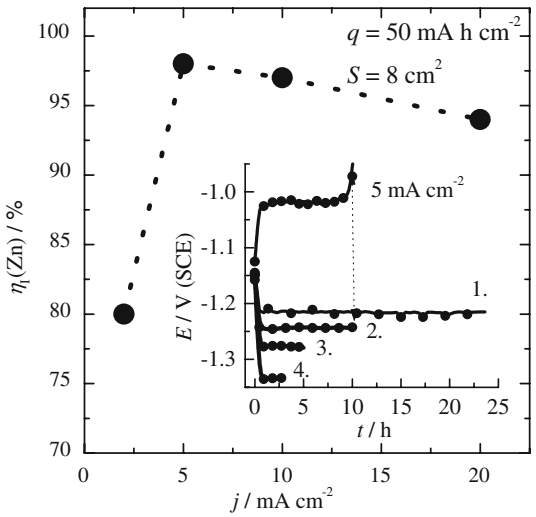

Fig. 4 Determined current efficiency of zinc deposition reaction on the copper electrode for the different deposition current densities. Inset: galvanostatic curves for zinc deposition at current densities of (1) 2, (2) 5, (3) 10, and (4) 20 mA cm^{-2} and for dissolution at a current density of 5 mA cm^{-2}

These results could be connected with the morphology of zinc deposits, shown in Fig. 5. A deposit obtained at a relatively small current density (2 mA cm^{-2}) was coarse and porous, with a lot of cavity induced by hydrogen evolution. Further increase of current density to 5 mA cm^{-2} and above, coarsens the deposit and decreases its porosity.

It should be noted that at the dendrite formation was not observed in any current density, even when the deposition charge was ~5 times higher than that in the pure chloride electrolyte (see Fig. 2).

3.1.3 Mechanism of the zinc deposition reaction

Considering the polarization measurements, deposition current efficiency, and morphology, the following mechanism for zinc deposition reaction could be suggested.

At pH ~5 in the presence of citrate in solution, zinc ion forms different types of complex with suggested species [19]:

$$Zn^{2+} + HCit^{2-} = ZnHCit \quad (pK_s = 3.0) \tag{4}$$

$$Zn^{2+} + Cit^{3-} = ZnCit^{-} \quad (pK_s = 4.8) \tag{5}$$

$$ZnCit^{-} + Cit^{3-} = ZnCit_2{}^{4-} \quad (pK_s = 1.7). \tag{6}$$

Due to the values of stability constants, it could be suggested that the main species in the solution was $ZnCit^{-}$, and the concentration of ZnHCit is considerably smaller, while the concentration of $ZnCit_2{}^{4-}$ and free zinc ions are rather low. Since deposition current density and potential depend on the concentration of the reacting species, decreasing the concentration provokes the decrease of the deposition current density, and at some point, the limiting current could be observed. Hence, the few waves in the cathodic part of the polarization curve (Fig. 3) could be assigned to the reduction of different species from the solution.

According to this analysis, it could be suggested that at relatively low current densities (~2 mA cm^{-2}), simultaneous deposition of zinc (~80%) from less stable complex or free zinc ion and hydrogen evolution (~20%) from protonated citrate species occurred, for example, via the following reactions:

$$2HCit^{2-} + 2e = H_2 + 2Cit^{3-} \tag{7}$$

$$Zn^{2+} + 2e = Zn \tag{8}$$

$$ZnCit_2{}^{4-} + 2e = Zn + 2Cit^{3-}. \tag{9}$$

Further increase of the current density (~5–15 mA cm^{-2}) leads to increases of the zinc deposition rate from more stable complex forms, such as

$$ZnHCit + 2e = Zn + HCit^{2-}, \tag{10}$$

or more probably,

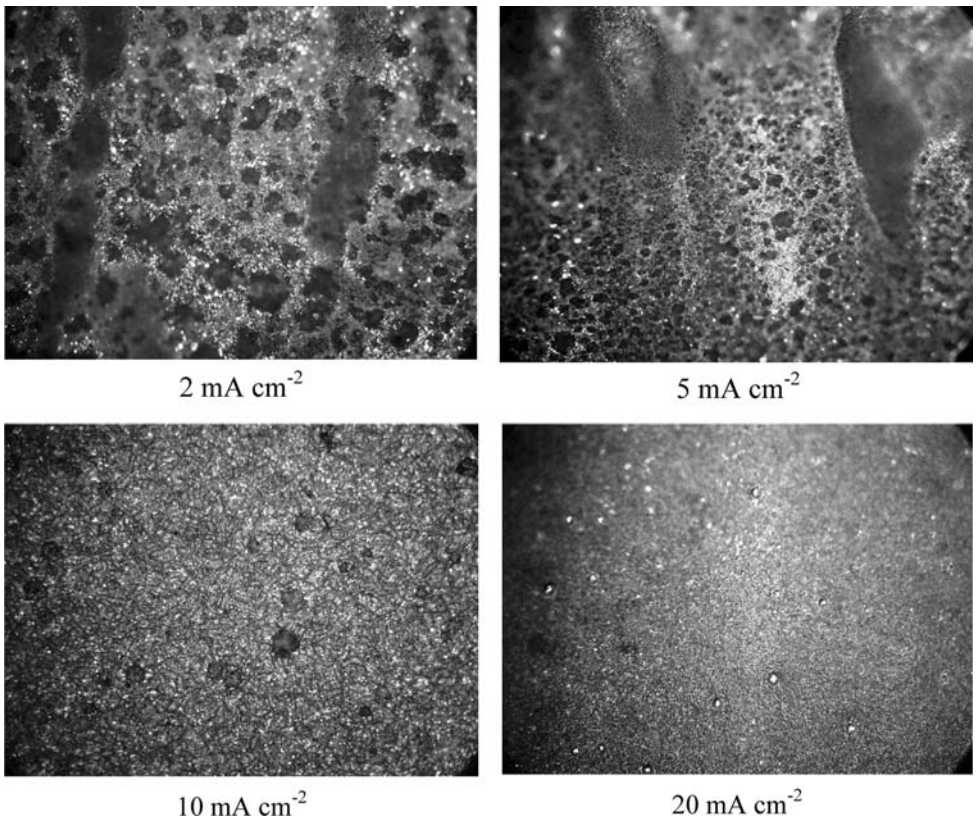

Fig. 5 Micrographs of the zinc deposits for different current densities in citrate/chloride-contained electrolyte, magnification 100×

$$ZnCit^{-} + 2e = Zn + Cit^{3-}. \quad (11)$$

At the same time, the hydrogen evolution rate from protonated citrate species, which is now under the domination of limiting current, tends to much lower potentials, and practically does not affect the current efficiency. For the current density of 20 mA cm^{-2} and above, due to the negative potentials, the possibilities of hydrogen evolution from water molecule now exists, which influence further decrease of the zinc deposition current efficiency.

Considering the presented analysis, it could be suggested that some optimum zinc deposition current densities (battery charge) lie in the range of ~5–15 mA cm^{-2}. On the other hand, any anodic current density (battery discharge) in the range of 0.5 up to 30 mA cm^{-2} could be applied.

3.2 Polyaniline electrode

On the basis of determined "optimum composition of the electrolyte" for the zinc electrode, the electrochemical behavior of PANI electrode in the same electrolyte was investigated. Figure 6 shows galvanostatic curve of the aniline polymerization from the solution containing 1 M HCl and 0.25 M aniline monomer on graphite electrode at a current density of 2 mA cm^{-2} with a polymerization charge of 0.6 mA h cm^{-2}. Polymerization starts at the potential of ~0.6 V and proceeds in the potential range between 0.72 and 0.68 V.

After polymerization, electrode with 1 mA cm^{-2} was discharged, washed with bidistilled water, and transferred into the three-compartment electrochemical cell with chloride/citrate electrolyte. After transfer, the electrode

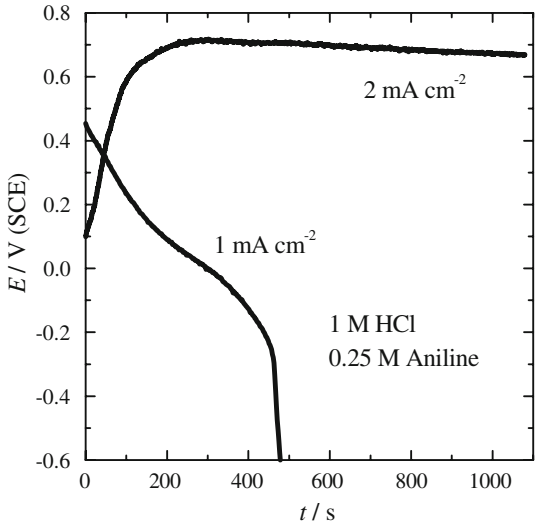

Fig. 6 Galvanostatic curves (2 mA cm^{-2}) for the aniline polymerization and discharge (1 mA cm^{-2}) in the solution containing 1 M HCl and 0.25 M aniline on graphite electrode

was conditioned at a potential of −0.6 V for 600 s to be completely discharged.

Figure 7 shows typical charge/discharge curves of PANI electrode for the different current densities. The potentials were limited to 0.35 V for charge and to –0.3 V for discharge. Charge of the discharged PANI electrode starts in the potential range between ∼−0.1 and ∼0.02 V depending on the applied current density. Potential increases practically linearly up to 0.35 V. Discharge of the electrode occurred in the potential range between ∼0.3 and ∼0.2 V with an average discharge potential of ∼0 V. For the potentials more negative than −0.2 V, diffusion limitations provoke the sharp decrease of the potentials.

Times of charge/discharge for different current densities determined from Fig. 7 are shown in Fig. 8. Calculated Columbic efficiency for the charge/discharge, shown in the inset of Fig. 8, was affected with the applied current density.

Assuming the limitations of anion diffusion through polymer film, it was possible to extrapolate the maximum electrode capacity by plotting the reciprocal square root values of the determined electrode capacity (shown in the inset of Fig. 9) with applied current densities. As it can be seen in Fig. 9, the determined maximum electrode capacity (q_0) of PANI electrode was ∼0.15 mA h cm^{-2}. On the other hand, some operating electrode capacity was in the range of 0.08–0.13 mA h cm^{-2} depending on the applied current density. All the investigated current densities (0.75–3 mA cm^{-2}) could be applied, but lower values will be favorable due to the higher capacity and Columbic efficiency.

Charge/discharge curves at a constant current density of 1 mA cm^{-2} versus the cycle number were shown in Fig. 10. The cycling potentials were limited to 0.35 V for charging and to −0.6 V for discharging. As it can be

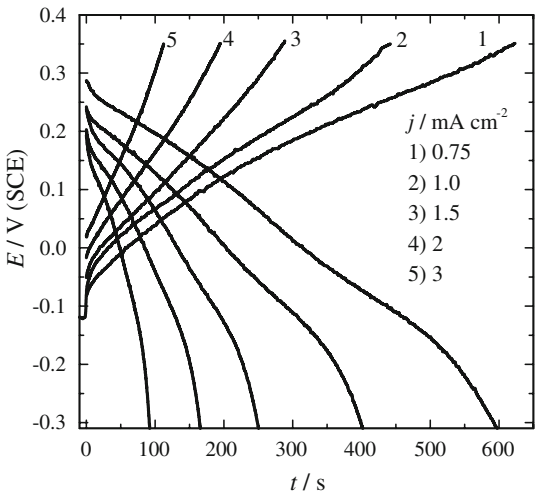

Fig. 7 Charge/discharge curve of the PANI electrode in citrate/chloride electrolyte for different current densities (marked in figure)

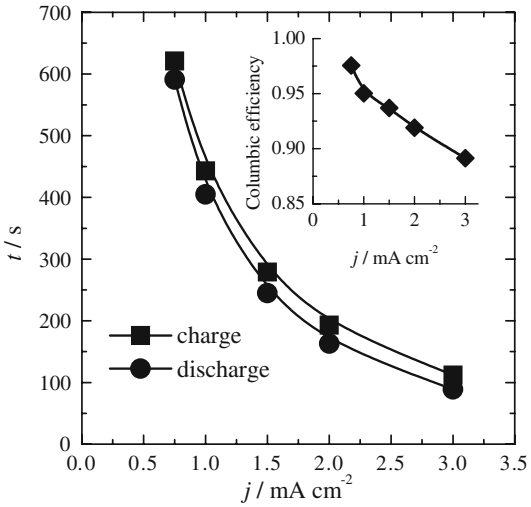

Fig. 8 Times of charge/discharge reaction determined for different current densities. Inset: dependence of columbic efficiency during charge/discharge on the applied current density

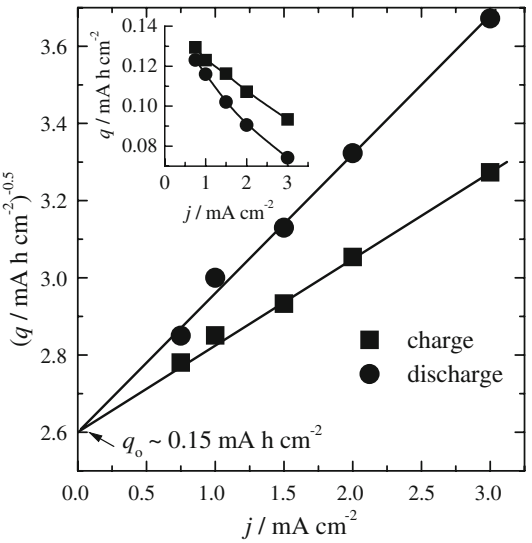

Fig. 9 Dependence of the reciprocal square root values of the electrode capacity (shown in the inset) on applied current densities

observed during the twenty cycles, the electrode capacity practically has a constant value without degradation. The same could be concluded from the cyclic voltammograms, shown in the inset of Fig. 10, since before the first and after twenty cycles, there were no changes in the shape of the voltammograms.

3.3 Possible characteristics of the real cell

Considering the above presented results for the zinc and PANI electrode in the optimum composition of the electrolyte, the possible electrochemical characteristics of

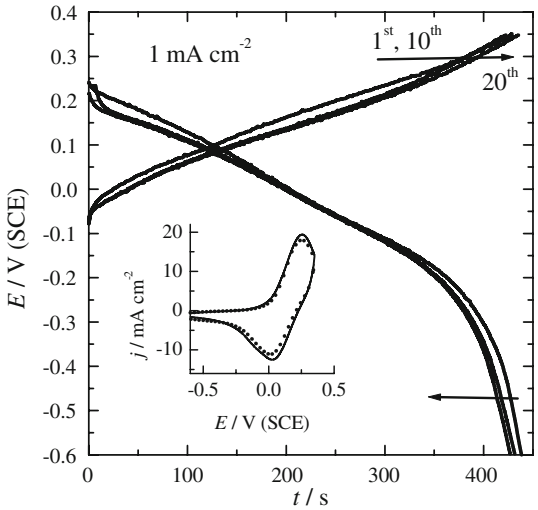

Fig. 10 Charge/discharge curve at a constant current density (1 mA cm^{-2}) versus cycle number in citrate/chloride electrolyte for the anodic potential limit of 0.35 V. Inset: cyclic voltammograms ($v = 20$ mV s^{-1}) of PANI electrode before first (—) and after twenty cycles (·····)

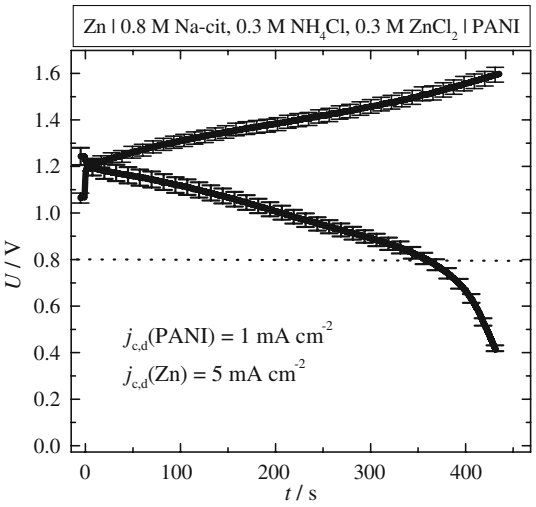

Fig. 11 Simulation of the possible charge/discharge characteristic of Zn|PANI cell in citrate/chloride-contained electrolyte

Zn|PANI secondary cell necessary for the cell optimization was discussed and simulated.

The Zn | 0.8 M Na-citrate, 0.3 M NH_4Cl, and 0.3 M $ZnCl_2$ | PANI electrochemical system will be mainly based on the following half-cell reactions:

$$[\mathrm{PANI}]_n + ny\mathrm{Cl}^- \underset{\text{Discharge}}{\overset{\text{Charge}}{\rightleftarrows}} \left[\mathrm{PANI}^{y+}(\mathrm{Cl}^-)_y\right]_n + nye \quad \text{(Positive electrode)}, \tag{12}$$

where y is doping degree, and

$$\mathrm{ZnCit}^- + 2e \underset{\text{Discharge}}{\overset{\text{Charge}}{\rightleftarrows}} \mathrm{Zn} + \mathrm{Cit}^{3-} \quad \text{(Negative electrode)}. \tag{13}$$

The reactions during charge/discharge of the complete cell will be as follows:

$$2[\mathrm{PANI}]_n + 2ny\mathrm{Cl}^- + ny\mathrm{ZnCit}^- \underset{\text{Discharge}}{\overset{\text{Charge}}{\rightleftarrows}} 2\left[\mathrm{PANI}^{y+}(\mathrm{Cl}^-)_y\right]_n + ny\mathrm{Zn} + ny\mathrm{Cit}^{3-} \tag{14}$$

The citrate anion was not considered as a doping anion for the PANI electrode during charge, because it was suggested that at less positive potentials, doping proceeds with chloride and at the more positive potentials (>0.35 V) with citrate anions, where faster degradation could occur [15].

It should be noted that the cell has to be formed in the discharged state.

For the given optimum composition of the electrolyte, the operating current densities will be in the range of ~0.75–3 mA cm^{-2} for the PANI electrode and 5–15 mA cm^{-2} for the zinc electrode. Due to the differences in the current densities, the area of PANI electrode should be at least five times higher than that for the zinc plate electrode. On that manner, Fig. 11 shows the simulation of charge/discharge curve with possible errors, for the complete Zn|PANI cell in chloride/citrate electrolyte for the current density of 1 mA cm^{-2} for PANI and 5 mA cm^{-2} for the zinc electrode. Data were extrapolated from Figs. 4 and 10, and simulation was done according to the procedure given in [20].

As it can be seen from Fig. 11, charge of the cell will occur in the voltage range between ~1.05 and ~1.62 V. After charge, the open circuit voltage will be ~1.25 V. Discharge will occur at the voltage range between 1.2 and ~0.4 V, with the most of the capacity (~85%) delivered above 0.8 V.

4 Conclusion

By investigating the polarization characteristic of the zinc deposition/dissolution reaction and corrosion rate from electrolytes containing 0.8 M sodium citrate, 0.3 M ammonium chloride, and different concentrations of zinc chloride (0.05–0.5 M), it was suggested that there will be some optimum electrolyte composition with ~0.3 M of zinc chloride.

Based on the determined deposition current efficiency and morphology of zinc deposits, it was suggested that some optimum deposition (charge) current density will be in the range of ~5–15 mA cm^{-2}.

In the optimum electrolyte, PANI electrode shows satisfactory characteristics for potential application as a positive electrode in the Zn|PANI secondary cell. Operating electrode

capacity in the range of 0.8 to 0.13 mA h cm^{-2} depending on the applied current density (0.75–3 mA cm^{-2}) was determined. All the investigated current densities could be applied, but lower values will be favorable due to the higher electrode capacity and Columbic efficiency.

According to the differences in the electrodes optimum current densities, the area of the PANI electrode should be at least five times higher than that for the zinc electrode.

By the simulation of the charge/discharge characteristic of the real cell, it was suggested that charge will occur in the voltage range between $\sim$1 and $\sim$1.6 V. After charge, the open circuit voltage will be $\sim$1.25 V, and discharge will occur in the voltage range between 1.2 and $\sim$0.4 V, with the most of the capacity ($\sim$85%) delivered above 0.8 V.

Acknowledgment This study is financially supported by the Ministry of Science and Environmental Protection, Republic of Serbia, contract No. 142044.

References

1. Rüetschi P (1993) J Power Sourc 42:1
2. Beck F, Rüetschi P (2000) Electrochim Acta 45:2467
3. Novák P, Müller K, Santhanam KSV, Haas O (1997) Chem Rev 97:207
4. Kaya M, Kitani A, Sasaki K (1984) Denki Kagaku 52:847
5. Kitani A, Kaya M, Sasaki K (1986) J Elecrochem Soc 133:1069
6. Sima M, Visan T, Buda M (1995) J Power Sourc 56:133
7. Mirmohseni A, Solhjo R (2003) Eur Polym J 39:219
8. Kan J, Xue H, Mu S (1998) J Power Sourc 74:113
9. Shaolin Mu (2004) Synth Metals 143:269
10. Mengoli G, Musiani MM, Pletcher D, Valcher S (1987) J Appl Electrochem 17:515
11. Rahmanifar MS, Mousavi MF, Shamsipur M, Ghaemia M (2004) J Power Sourc 132:296
12. Rahmanifar MS, Mousavi MF, Shamsipur M, Heli H (2005) Synth Metals 155:480
13. Ghanbari K, Mousavi MF, Shamsipur M, Karami H (2007) J Power Sourc 170:513
14. Xinsheng W, Xin J, Dawei GU, Linjiang S (2006) Rare Metals 25:67
15. Jugović BZ, Trišović TLj, Stevanović JS, Maksimović MD, Grgur BN (2006) Electrochim Acta 51:6268
16. Jugović BZ, Trišović TLj, Stevanović JS, Maksimović MD, Grgur BN (2006) J Power Sourc 160:1447
17. Marinović V, Despić AR (1997) J Electroanal Chem 431:127
18. Stanković S, Grgur B, Krstajić N, Vojnović M (2003) J Electroanal Chem 549:37
19. Berthon G, May PM, Williams DR (1978) J Chem Soc Dalton Trans 1433
20. Grgur BN, Ristić V, Gvozdenović MM, Maksimović MD, Jugović BZ (2008) J Power Sourc 180(1):635